Structure and Thermal Expansivity of Tetrahydrofuran Deuterate Determined by Neutron Powder Diffraction

ARTICLE *in* THE JOURNAL OF PHYSICAL CHEMISTRY B · JUNE 2003

Impact Factor: 3.3 · DOI: 10.1021/jp020513n

ARTICLES

Structure and Thermal Expansivity of Tetrahydrofuran Deuterate Determined by Neutron Powder Diffraction

C. Y. Jones,*,† S. L. Marshall,† B. C. Chakoumakos,† C. J. Rawn,† and Y. Ishii‡

Oak Ridge National Laboratory, Oak Ridge, Tennessee 37831, and Japan Atomic Energy Research Institute, Tokai-mura, Naka-gun 311-1195, Japan

Received: February 25, 2002; In Final Form: January 10, 2003

The crystal structure of tetrahydrofuran deuterate, a clathrate hydrate, has been refined from neutron powder diffraction data at five temperatures in the range 7−265 K. The thermal expansivity was shown to be greater than that of ice I*h* in the same range of temperature (*T*), as observed in previous studies of other clathrates. The overall effect of *T* has been resolved into contributions from different geometrical parameters in the structure. Thus, an increase in *T* results in expansion of the host-lattice framework with increases in both the D−D and O−O distances and out-of-plane tilting of water molecules. The greatest dependence on *T* is exhibited by the D−D distances and the distortion of the hexagonal faces from planarity, which is particularly pronounced in the range 75−140 K. The cage volumes show a complex dependence on *T*: from 7 to 140 K, the volume of the small cage decreases slightly and that of the large cage increases, and between 140 and 205 K, the trend is reversed. The most pronounced structural changes occur in a similar regime of *T* as changes in guest dynamics observed in spectroscopic and thermodynamic studies. The temperature dependences of the structure and $\alpha(T)$, when considered along with the relation of $\alpha(T)$ to the degree of anharmonicity in bonding,[34] could be formulated to provide a sensitive test of molecular models of clathrate hydrates.

Introduction

In recent years, studies of natural gas hydrates have been motivated by their potential as an energy source and have dominated research interests in the class of water-based inclusion compounds known as clathrate hydrates. However, numerous experimental and theoretical studies of tetrahydrofuran (THF) hydrate and other easily synthesized clathrate hydrates have also yielded information regarding the crystal structures and guest−host/guest−guest interactions. THF hydrate (THFH), $C_4H_8O\cdot nH_2O$ ($16 < n < 17$), is a structure II (sII) clathrate hydrate that contains a large guest molecule, THF, with a permanent dipole. Diffraction studies of THF and other hydrates have provided models of the host structure and descriptions of the orientational disorder of the guest molecules. The structure of the THFH was first determined in 1958 by X-ray powder diffraction by von Stackelberg and Meuthen[1] and later confirmed by Sargent and Calvert.[2] A more detailed structural analysis of THF−hydrogen sulfide (H_2S) hydrate from X-ray diffraction data was carried out by Mak and McMullan.[3] By means of a Fourier difference synthesis, they observed a spherical shell of electron density with a radius, *r*, of 1.1 Å at the center of the large cage and assigned this to the THF molecule. In a more recent neutron-diffraction study of potassium hydroxide-doped THF deuterate (THFD) at 5 and 80 K, Yamamuro et al.[4] determined the crystal symmetry to be tetragonal at 5 K.

For THFH, heat capacity,[5−9] enthalpies of dissociation[6] and fusion,[7] and thermal conductivity[5,10] have been determined and interpreted in terms of contributions due to either the host or the THF molecules. In addition, dynamics of THFH have been studied directly by dielectric relaxation measurements[11−13] and infrared,[14] Raman,[15] and NMR spectroscopies.[16,17] These studies revealed a distribution of relaxation times ascribed to the disorder of the host water molecules and characterized the orientational motion of guest molecules as hindered rotation that becomes essentially free at $T \approx 100$ K.

In the present paper, we report Rietveld refinements of neutron powder diffraction data on undoped THFD over an extended temperature range, 7−265 K. From these data, we derive the thermal expansivity, $\alpha(T)$, and describe the temperature dependence of the host structure. The thermal expansivity of THFH, and clathrate hydrates in general, is of scientific interest in the elucidation of the effect of guest molecules on the thermal expansivity. From a technological perspective, the current interest in natural gas hydrates as potential sources of energy warrants a detailed, systematic study of the structural and thermophysical properties of clathrate hydrates over wide ranges of composition, temperature, and pressure.

Experimental Section

Sample Preparation and Measurements. THFD was prepared by mixing stoichiometric amounts of THF (Aldrich, 99.999%) and deuterium oxide (Aldrich, 99.999%) and immersing the mixture in liquid nitrogen. The frozen sample was crushed to a powder, transferred to a thin-walled vanadium can

* To whom correspondence should be addressed. Presently at the National Institute of Standards and Technology, 100 Bureau Drive, Gaithersburg, MD 20899. E-mail: camille.jones@nist.gov.
† Oak Ridge National Laboratory.
‡ Japan Atomic Energy Research Institute.

10.1021/jp020513n CCC: $25.00
Published on Web 06/03/2003

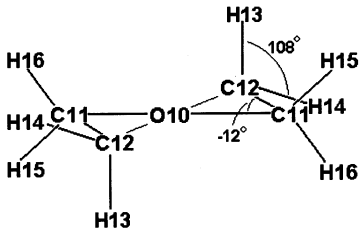

Figure 1. Approximate conformation of THF used for the rigid-body refinement.

(6 cm × 1.5 cm i.d.), sealed inside with an indium-gasketed lid, and stored in dry ice until the experiment. The sample can containing ~8 g of powder was mounted on the cold tip of a closed-cycle He refrigerator and data were collected on the high-resolution powder diffractometer (HRPD) on the JRR-3M research reactor at the Japan Atomic Energy Research Institute (JAERI) in Tokai, Japan. A wavelength of 1.1635 Å, calibrated with a Si standard, was used. Data were collected for approximately 9 h each at 7, 75, 140, 205, and 265 K with 64 detectors accessing $5° < 2\theta < 165°$, a step size of 0.05°, and a counting time of 600 s per step. The temperature of the sample was measured with a silicon diode sensor at the top of the sample can. The temperature gradient across the sample was ~1 K. Transmission was measured through a 1 × 30 mm^2 slit placed with and without the sample and CCR for the calculation of a Debye−Scherrer absorption correction.[18] A transmittance of 0.84 was obtained for the THFD sample in a vanadium can with a packing density of 0.5 g cm^{-3}. This value corresponds to $\mu r = 0.17$, where μ is the linear absorption coefficient in cm^{-1} and r is the inner radius of the can in cm.

Structure Refinement. Rietveld refinement was performed with the General Structure Analysis System (GSAS) suite of programs.[19] Neutron scattering lengths, $\bar{b}$, were those from the tabulation of Sears.[20] Refinements were performed on total intensity vs 2θ. The initial crystal structure model for the sII host lattice was taken from Mak and McMullan.[3] The initial atom coordinates differ from theirs by a translation ($-1/8$, $-1/8$, $-1/8$) to give setting 2 for the space group $Fd\bar{3}m$.

The coordinates of the THF guests were determined from plots of observed Fourier (FOBS) and difference Fourier (DIFF) maps. The THF molecule itself was modeled as a rigid body (RB), and its geometry was based on the structure obtained from a refinement of high-resolution neutron powder diffraction data on deuterated THF at 5 K.[21] The most stable conformation of THF, shown in Figure 1, is a twist form with C_2 symmetry. The internal coordinates for the RB are listed in Table 1. The xy plane of the internal coordinate system was defined to coincide with the C11−O10−C12 plane of the THF molecule. For refinement, the RB was reoriented by performing the rotation ($-\pi/4$, 0, $3\pi/4$) so that the C_2 axis of THF was perpendicular to a hexagonal face of the hexakaidecahedron. The initial orientation of the RB was taken from Davidson,[22] who suggested that the O atom of THF is more easily accommodated when oriented toward the center of a hexagonal face.

Refinement was performed on diffractometer zero, background (a 12-term Chebyshev polynomial), peak profiles (Gaussian with asymmetry), lattice parameters, atom positions, isotropic atomic displacement parameters (U_{iso}), and an isotropic RB displacement parameter. The U_{iso} values for host-lattice O atoms were constrained to be identical; the same constraint was applied to all D atoms. The displacement parameter for the RB was obtained by refinement of translational and librational matrices in the TLS formalism.[23] Isotropic translational, T_{iso}, and librational, L_{iso}, displacement parameters were refined in separate trials. When released, a constrained occupancy factor on THF refined to unity within its estimated uncertainty, consistent with previous studies,[22,24,25] and was later held constant at unity. A second phase, D_2O ice Ih, was included in the refinement. The structure models used for ice were those of Peterson and Levy[26] at 123 and 223 K; only lattice parameters were refined. The weight fraction of D_2O refined to values in the range 9−15%; a value of 12% was assigned at all temperatures.

TABLE 1: Internal Coordinates for the THF RB, Shown in Figure 1[a]

atom	vector	x	y	z
O10	t_1	0	0.871	0
	t_2	0	0	0
C11	t_1	0.827	0.271	0
	t_2	0	0	0
C12	t_1	0.544	−0.679	0.1
	t_2	0	0	0
H13	t_1	0.827	0.271	0
	t_2	0.827	0.271	0.93
H14	t_1	0.827	0.271	0
	t_2	0.827	0.271	−0.84
H15	t_1	0.544	−0.679	0.1
	t_2	0.544	−0.679	−0.1
H16	t_1	0.544	−0.679	0.1
	t_2	0	0	1

[a] The magnitude of translation vector 1, t_1, is 1.24 Å and t_2 is 1.097 Å. The coordinates were calculated from the following expressions: 0.871 = 1/(2 cos 54.95°), 0.827 = (sin 71.85°)/(2 cos 54.95°), 0.271 = (cos 71.85°)/(2 cos 54.95°); 0.544 = (cos 51.3°)/(2 cos 54.95°); −0.679 = (sin 51.3°)/(2 cos 54.95°); −0.84 = 1.097(sin −50°).

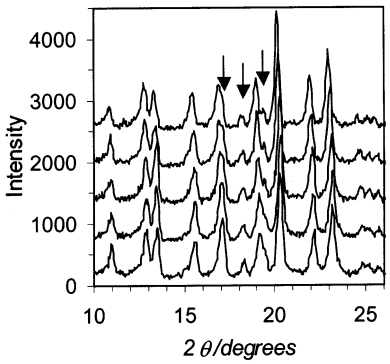

Figure 2. Low-angle region of diffractograms measured at (bottom to top) 7, 75, 140, 205, and 265 K. Reflections from ice Ih are indicated by the arrows; the first reflection at ~17.5° is unresolved from the larger clathrate hydrate reflection at that location.

Results

Thermal Expansivity. All of the observed reflections were accounted for by THFD and D_2O ice Ih. Small changes in both the positions and intensities were observed in the diffraction patterns, shown in the low-angle region in Figure 2. Refined lattice parameters for these two phases are listed in Table 2. The lattice parameter of THFD, plotted in Figure 3, exhibits a nonlinear dependence on T. Becausee $\alpha(T)$ is defined in terms of a relative increase in molar volume and because the thermal expansion of THFD is isotropic, it is appropriate to characterize the temperature dependence of the lattice parameter by a relation of the form

$$10^5 \ln \frac{a}{a_o} = c_1[(T - T_o)/K] + c_2[(T - T_o)/K]^2 \qquad (1)$$

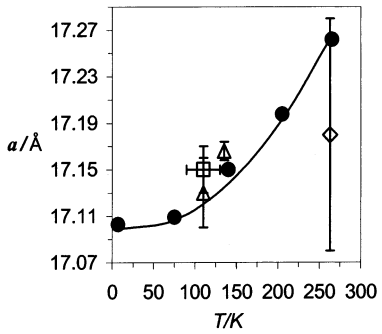

Figure 3. Temperature dependence of the lattice parameter for THFD. The error bars are smaller than the symbols themselves. Lattice parameters on THF hydrate obtained from the literature are also plotted: (◊) von Stackelberg and Meuthen[1]; (□) Bertie and Jacobs;[14] (△) Sargent and Calvert.[2]

TABLE 2: Lattice Parameters for THFD and Ice I*h*

	THFD	D_2O	
T (K)	a (Å)	a (Å)	c (Å)
7	17.103(2)	4.490(1)	7.315(2)
75	17.109(1)	4.490(1)	7.315(2)
140	17.150(1)	4.495(1)	7.319(3)
205	17.198(2)	4.501(1)	7.332(3)
265	17.262(1)	4.518(1)	7.347(3)

where T_o is 7 K and $a_o = a(T_o) = 17.103$ Å, which leads to a linear dependence of $\alpha(T)$ on the difference $T - T_o$. The adjustable parameters c_1, c_2, and the correct temperature values were estimated simultaneously by generalized least squares.[27,28] Assuming standard deviations of 0.002 Å and 1 K for $a(T)$ and T, respectively, the parameter estimates are $c_1 = -0.454(0.329)$ and $c_2 = 0.0163(0.002)$, and the combined weighted sum of squared residuals for the fit was 192. The parameter estimates have large standard errors but are both statistically significant. In contrast, the use of conventional, unweighted least squares—neglecting the uncertainty in T—leads to a statistically insignificant estimate for c_1. As shown in Figure 3, the assumed functional relationship reproduces the trend in the data, but there are insufficient data to allow meaningful estimates to be made of a_o as a third adjustable parameter.

Estimates for $\alpha(T)$ were obtained by differentiation of the integrated expression in eq 1 with respect to T. For example, at 100, 150, and 250 K, values for $\alpha(T)$ are $28.1(4) \times 10^{-6}$, $44.4(6) \times 10^{-6}$, and $77.0(1.5) \times 10^{-6}$ K^{-1}, respectively. For comparison, the respective values for $\alpha(T)$ reported for THFH by Davidson et al.[29] are 36×10^{-6}, 45×10^{-6}, and 61×10^{-6} K^{-1} and display a weaker linear dependence on T. Values obtained from dilatometry[30] at the above temperatures are 28×10^{-6}, 42×10^{-6}, and 62×10^{-6} K^{-1}. Lattice parameters for ice refined in this study yield an $\alpha(T)$ of $11.5(4) \times 10^{-6}$, $20.5(6) \times 10^{-6}$, and $30(1) \times 10^{-6}$ K^{-1} along the c-axis at 100, 150, and 250 K, respectively. Refined lattice parameters for D_2O ice I*h* are systematically lower (by 0.01−0.02 Å) than values reported by Röttger et al.[31]

Clathrate Structures. Figure 4 shows the two types of cages and three types of faces found in the sII framework of THFD. The hexakaidecahedral (HEX) cage comprises hexagonal faces (HF1) with O3 atoms as vertexes and pentagonal faces (PF1) having one O2 atom and four O3 atoms as vertexes; its pentagonal face is shared with the dodecahedral (DOH) cages. A second type of pentagonal face (PF2), present only in the DOH cage, has atoms O1−O3 as vertexes and is shared by two DOH cages. The nuclear scattering-length density (density) in FOBS maps can be assigned to each type of cage and face,

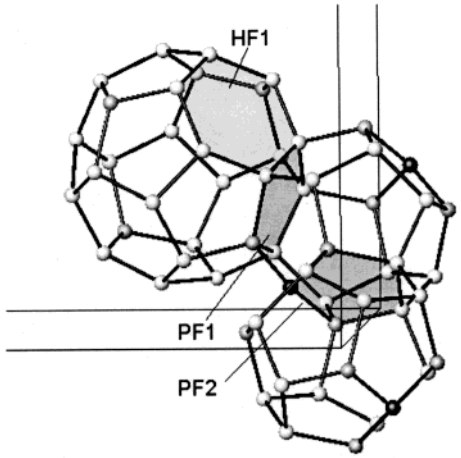

Figure 4. Relative locations of HEX and DOH cages in the unit cell of THFD viewed along [−0.992, −0.087, 0.087]. Atoms are as follows: O1, black; O2, dark gray; O3, light gray. Model drawn with ATOMS (Shape Software).

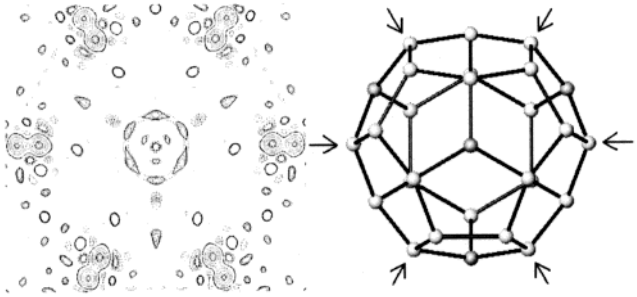

Figure 5. FOBS map of the HEX cage of THFD at 7 K viewed along and centered at ($^3/_8$, $^3/_8$, $^3/_8$). Contours are drawn at 0.5−10.0 fm. The nuclear density from THF lies at the broken ring of density at the center and has a maximum contour of 0.8 fm. The inner lobes of the peanut-shaped contours are O3, indicated by arrows in the accompanying drawing. The outer lobes are D7 or D8.

with a maximum residual density contour of 0.5 fm. The density at the guest positions is roughly an order of magnitude lower than that at the host-atom positions; given that $\bar{b}(D)/\bar{b}(O) \approx 1.1$, the map contour levels indicate that the D sites are half-occupied. A FOBS map of a cross section through the HEX cage, shown in Figure 5, contains a hexagonal array of density maxima corresponding to host atoms and a small broken ring of positive nuclear density with $r = 1.5$ Å centered at ($^3/_8$, $^3/_8$, $^3/_8$). Similar FOBS and DIFF maps through the centers of DOH cages show no evidence of nuclear density. The 15 density maxima in PF1 lie in a single plane across the entire temperature range; atoms in PF2 are constrained by symmetry to lie in a plane. In FOBS maps of HF1, the D atoms are located slightly above and below the plane of the ring of O atoms at 7 K; conversely, at 265 K, the average position of the D atoms lie in a plane and the O atoms lie out of this plane. Also, as T increases, the density maxima of the D atoms decrease and the density spreads out perpendicular to the hexagon and to a lesser extent in the plane of the hexagon.

Atomic coordinates for THFD are listed in Table 3; the coordinates of the host atoms agree with those reported by Mak and McMullan.[3] In both their work and the present work, the H atom at the general position on the hexagonal face (D9 in this work) rests out of the plane, whereas the remaining atoms lie in the plane, that is, on or close to the polyhedron edges. As T increases, the average O−D bond distance and O−O−O bond angles remain constant. However, in general the D−O−D bond angle the D−D and O−O distances increase; the D8−D8

TABLE 3: Atom Parameters for the D_2O Host Lattice and THF Guest Molecules

atom	*x*	*y*	*z*	*f*	symm	multipl
			D_2O Host Lattice			
			7 K			
O1	1/8	1/8	1/8	1	$\bar{4}3m$	8
O2	0.2196(9)	0.2196(9)	0.2196(9)	1	3*m*	32
O3	0.1822(5)	0.1822(5)	0.3719(9)	1	*m*	96
D4	0.1838(13)	0.1838(13)	0.1838(3)	0.5	3*m*	32
D5	0.1618(11)	0.1618(11)	0.1618(11)	0.5	3*m*	32
D6	0.2046(1)	0.2046(1)	0.2700(13)	0.5	*m*	96
D7	0.1969(12)	0.1960(12)	0.3133(14)	0.5	*m*	96
D8	0.1414(8)	0.1414(8)	0.3676(15)	0.5	*m*	96
D9	−0.1647(10)	−0.0210(9)	0.1483(9)	0.5	1	192
			75 K			
O1	1/8	1/8	1/8			
O2	0.2187(8)	0.2187(8)	0.2187(8)			
O3	0.1821(4)	0.1821(4)	0.3720(7)			
D4	0.1859(11)	0.1859(11)	0.1859(11)			
D5	0.1608(9)	0.1608(9)	0.1608(9)			
D6	0.2051(9)	0.2051(9)	0.2689(11)			
D7	0.1946(9)	0.1946(9)	0.3126(12)			
D8	0.1421(7)	0.1421(7)	0.3687(12)			
D9	−0.1624(8)	−0.0230(8)	0.1471(8)			
			140 K			
O1	1/8	1/8	1/8			
O2	0.2186(8)	0.2186(8)	0.2186(8)			
O3	0.1798(4)	0.1798(4)	0.3713(8)			
D4	0.1862(11)	0.1862(11)	0.1862(11)			
D5	0.1622(10)	0.1622(10)	0.1622(10)			
D6	0.2069(9)	0.2069(9)	0.2690(12)			
D7	0.1963(10)	0.1963(10)	0.3104(13)			
D8	0.1417(7)	0.1417(7)	0.3702(13)			
D9	−0.1685(9)	−0.0197(8)	0.1417(7)			
			205 K			
O1	1/8	1/8	1/8			
O2	0.2207(10)	0.2207(10)	0.2207(10)			
O3	0.1817(6)	0.1817(6)	0.3734(10)			
D4	0.1862(14)	0.1862(14)	0.1862(14)			
D5	0.1589(11)	0.1589(11)	0.1589(11)			
D6	0.2041(12)	0.2041(12)	0.2718(14)			
D7	0.1971(13)	0.1971(13)	0.3168(15)			
D8	0.1424(9)	0.1424(9)	0.3669(15)			
D9	−0.1677(11)	−0.0223(11)	0.1454(11)			
			265 K			
O1	1/8	1/8	1/8			
O2	0.2213(9)	0.2213(9)	0.2213(9)			
O3	0.1795(6)	0.1795(6)	0.3732(10)			
D4	0.1873(13)	0.1873(13)	0.1873(13)			
D5	0.1579(10)	0.1579(10)	0.1579(10)			
D6	0.2047(12)	0.2047(12)	0.2741(13)			
D7	0.1982(11)	0.1982(11)	0.3229(14)			
D8	0.1425(9)	0.1425(9)	0.3626(15)			
D9	−0.1710(10)	−0.0233(10)	0.1465(10)			
			THF Guest			
O10	0.4198	3/8	0.3302	0.0833	*m*	96
C11	0.4315	3/8	0.4036	0.1667	*m*	96
C12	0.3681	3/8	0.4379	0.0833	1	192
H13	0.4814	0.4348	0.4289	0.0833	1	192
H14	0.4814	0.3210	0.4289	0.0833	1	192
H15	0.3633	0.3686	0.4949	0.0833	1	192
H16	0.3681	0.4393	0.4379	0.0833	1	19

distance remains relatively constant. The D9−D9 intersite distance, plotted in Figure 6, and the distortion of the hexagonal face showed the greatest sensitivity to changes in *T*. The hexagonal face exhibits a marked distortion from planarity at ∼100 K, as plotted in Figure 7.

The volumes of the small and large cages as defined by the O-atom positions were computed with the program VINCI.[32] The volume of the small, 20-atom cage (V_{20}) was computed by decomposition of the cage volume into pentagonal pyramids defined by PF1, PF2, and the cage center at (0, 0, 0). The volume of the large, 28-atom cage (V_{28}) was then calculated from the

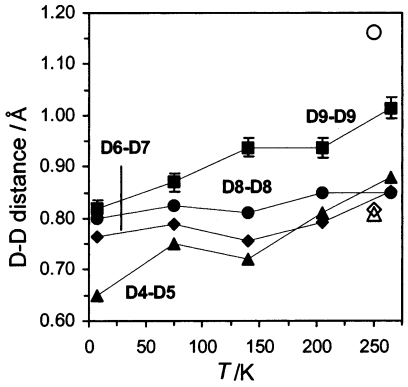

Figure 6. Temperature dependence of the D−D distances. Open symbols are the corresponding distances in THF−H_2S hydrate.[3]

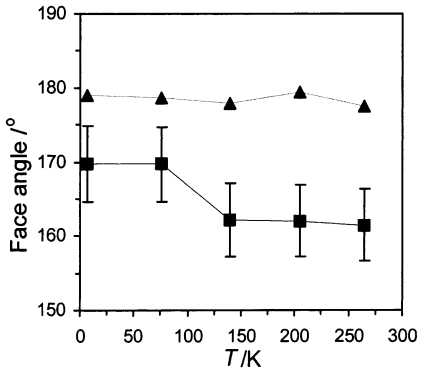

Figure 7. Temperature dependence of the HF1 (■) and PF1 (▲) face-bending angles.

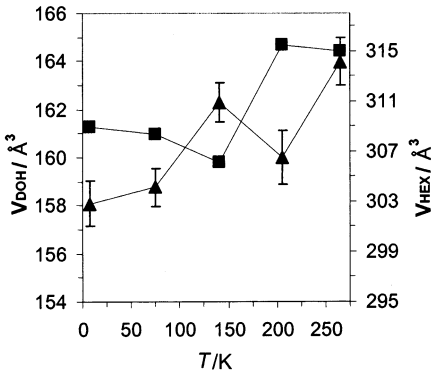

Figure 8. Volumes of the small (▲) and large (■) cages as a function of *T*.

TABLE 4: Atomic Displacement Parameters for D_2O and Libration Parameters for the THF RB

T (K)	U_{iso}(O) (Å)	U_{iso}(D) (Å)	L_{iso} (deg^2)
7	0.0172(12)	0.0148(9)	312(60)
75	0.0152(11)	0.0157(11)	266(49)
140	0.0232(16)	0.0179(12)	309(44)
205	0.0303(22)	0.0274(18)	321(49)
265	0.0404(31)	0.0348(23)	336(50)

relationship $V_{uc} = 16V_{20} + 8V_{28}$, where V_{uc} is the unit cell volume. From 7 to 140 K, V_{20} decreases slightly and V_{28} increases. Between 140 and 205 K, the trend reverses: V_{20} increases dramatically and V_{28} decreases. This behavior is in contrast to smooth increase in V_{uc} with *T*.

The atomic displacement parameters of the host atoms are listed in Table 4. Refinement of a single U_{iso} for both O and D host atoms yielded results statistically indistinguishable from their separate refinement. The value of U_{iso} for O at 265 K,

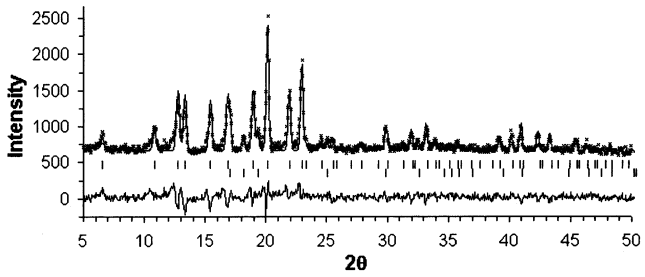

Figure 9. Refinement results for THFD at 265 K.

TABLE 5: Refinement Statistics for THFD

T (K)	wR_p	χ_r^2	no. of variables
7	6.05	2.34	20
75	6.00	2.13	30
140	5.98	2.12	31
205	5.82	2.17	31
265	5.67	1.88	37

0.0404(31) Å^2, is similar to the value, 0.044 Å^2, reported for THF−H_2S hydrate at 250−256 K.[3] For the RB, T_{iso} refined alone or T_{iso} and L_{iso} refined simultaneously yielded unstable refinements, but L_{iso} refined alone gave stable refinements and improved the statistics. The magnitude of L_{iso} refined to values in the range 437−639 deg^2 over the entire temperature range; this range of L_{iso} corresponds to a rms angular displacement of 20°−25°. The final refinement statistics are listed in Table 5, and a plot of the fit at 265 K is shown in Figure 9.

Discussion

Although disorder in clathrate hydrates precludes precise refinements of their crystal structures from constant-wavelength powder diffraction data, quantitative estimates of temperature-dependent changes in the host-atom structures are possible and generally support conclusions drawn from spectroscopic and thermodynamic studies. Further discussion focuses on HF1 and its distortions from planarity. This buckling of HF1 involves out-of-plane rotation of water molecules. The temperature dependences of the atomic coordinates of O3 and D9 are of particular interest because the HF1 faces are formed exclusively from these atoms. The largest change in the bending angle of HF1 occurs near the temperature at which heat-capacity measurements[18] indicate an onset of free-rotor-like behavior in the THF guests above 120 K. The O−O−O cage angles remain invariant, a result that is consistent with the results on methane hydrate in the range 2−150 K.[33] However, the D−O−D angles deviate from 109° as T increases. In addition, V_{20} and V_{28} display a complex dependence on temperature; however, although their sum must be equal to V_{uc}, their volumes do not necessarily have to follow the same volume expansion/contraction as the unit cell. If the O positions are influenced by the motion of the THF guest, then it may be possible to obtain more detailed correlations of cage volumes with the results from specific spectroscopic studies.

The maximum density contours in the FOBS maps at 7 K are greater than those at 75 K and above; this indicates greater disorder at higher temperatures. This observation is consistent with results of spectroscopic studies, in which motion in the range 15−60 K is observed to be more restricted than that in the range 60−225 K. Detailed structural studies of other sII clathrate hydrates may reveal systematic variations in the host structure with temperature and type of guest. For example, careful investigation of the degree of planarity of the cage faces as a function of T, P, or the occupancy or type of guest may provide additional insight as to the nature of the guest−host interactions. The temperature dependences of the structure and $\alpha(T)$, when considered along with the relation of $\alpha(T)$ to the degree of anharmonicity in bonding,[34] could be formulated to provide a sensitive test of molecular models of clathrate hydrates.

The present results show $\alpha(T)$ of THFD to be greater than that of ice I*h* in the same temperature range and of similar magnitude as that of the clathrate hydrates of CO_2,[35] CH_4,[33] and ethlyene oxide.[36] Therefore, the present results cannot be interpreted in terms of the theory that the large size of THF lowers the degree of anharmonicity of its vibrations and thus lowers $\alpha(T)$ of its hydrate relative to that of hydrates with smaller guests.[37] However, the standard errors in c_1 and c_2 are of the same order of magnitude as the parameters themselves. To obtain good agreement, it was necessary to assume small uncertainties in T; parameter estimates and their standard errors depend strongly on the uncertainty assumed for the temperature.

Conclusions

The structure of THFD has been refined over the range 7−265 K, and its thermal expansion has been described. Although the thermal expansion is isotropic, the atomic configuration of the host is sensive to changes in temperature. Thermal expansion occurs with progressive distortion of the hexagonal faces in the HEX cages. The cage volumes show a complex dependence on temperature; from 7 to 140 K, V_{20} decreases and V_{28} increases, and from 140 to 205 K, the trend is reversed. The results of this study concur with those of spectroscopic and calorimetric studies that show changes with T in the motions of the guest molecules. Careful attention during the collection of powder diffraction data to control temperature, optimize statistics, and minimize background and guest-atom scattering may allow specific correlations between structural features and dynamical properties to be identified.

Acknowledgment. Research was sponsored by the Laboratory Directed Research and Development Program of Oak Ridge National Laboratory (ORNL), managed by UT-Battelle, LLC for the U. S. Department of Energy under Contract No. DE-AC05-00OR22725, and by the Japan Atomic Energy Research Institute. The authors thank Eliot Specht and Yaspal Badyal for their helpful comments.

References and Notes

(1) von Stackelberg, M.; Meuthen, B. *Z. Elektrochem.* **1958**, *62*, 130−131.
(2) Sargent, D. F.; Calvert, L. D. *J. Phys. Chem.* **1966**, *70* (8), 2689−2691.
(3) Mak, T. C. W.; McMullan, R. K. *J. Chem. Phys.* **1964**, *42* (8), 2732−2737.
(4) Yamamuro, O.; Matsuo, T.; Suga, H.; David, W. I. F.; Ibberson, R. M.; Leadbetter, A. J. *Physica B* **1995**, *213−214*, 405−407.
(5) Ross, R. G.; Andersson, P. *Can. J. Chem.* **1982**, *60*, 881−892.
(6) Leaist, D. G.; Murray, J. J.; Post, M. L.; Davidson, D. W. *J. Phys. Chem.* **1982**, *86*, 4175−4178.
(7) Handa, Y. P. *Can. J. Chem.* **1984**, *62*, 1659−1661.
(8) White, M. A.; MacLean, M. T. *J. Phys. Chem.* **1985**, *89*, 1380−1383.
(9) Yamamuro, O.; Oguni, M.; Matsuo, T.; Suga, H. *J. Phys. Chem. Solids* **1988**, *49*, 425−434.
(10) Tse, J. S.; White, M. A. *J. Phys. Chem.* **1988**, *92*, 5006−5011.
(11) Davidson, D. W.; Davies, M. M.; Williams, K. *J. Chem. Phys.* **1964**, *40*, 3449−3450.
(12) Hawkins, R. E.; Davidson, D. W. *J. Phys. Chem.* **1966**, *70*, 1889−1894.
(13) Gough, S. R.; Hawkins, R. E.; Morris B.; Davidson D. W. *J. Phys. Chem.* **1973**, *77*, 2969−2976.
(14) Bertie, J. E.; Jacobs, S. M. *J. Chem. Phys.* **1978**, *69*, 4105.

(15) Tulk, C. A.; Klug, D. D.; Ripmeester, J. A. *J. Phys. Chem. A* **1998**, *102*, 8734−8739.
(16) Garg, S. K.; Davidson, D. W.; Ripmeester, J. A. *J. Magn. Reson.* **1974**, *15*, 295.
(17) Bach-Vergés, M.; Kitchin, S. J.; Harris, K. D. M.; Zugic, M.; Koh, C. A. *J. Phys. Chem. B* **2001**, *105* (14), 2699−2706.
(18) Hewat, A. W. *Acta Crystallogr.* **1979**, *A35*, 248.
(19) Larson, A. C.; Von Dreele, R. B. *General Structure Analysis System*; LAUR 86−748, Los Alamos National Laboratory: Los Alamos, NM.
(20) Sears, V. F. *Neutron News* **1992**, *3*, 26.
(21) David, W. I. F.; Ibberson, R. M. *Acta Crystallogr.* **1992**, *C48*, 301−303.
(22) Davidson, D. W. *Can. J. Chem.* **1971**, *49*, 1224−1242.
(23) Schomaker, V.; Trueblood, K. N. *Acta Crystallogr.* **1968**, *B24*, 63−75.
(24) Gough, S. R.; Davidson, D. W. *Can. J. Chem.* **1971**, *49*, 2691−2699.
(25) Rosso, J.-C.; Carbonnel L. *C. R. Acad. Sci.* **1971**, *C273*, 15−18.
(26) Peterson, S. W.; Levy, H. A. *Acta Crystallogr.* **1957**, *10*, 70−76.
(27) Lybanon, M. *Am. J. Phys.* **1984**, *52*, 22−26.
(28) Lybanon, M. *Comput. Geosci.* **1985**, *11*, 501−508.
(29) Davidson, D. W.; Handa, Y. P.; Ratliffe, C. I.; Ripmeester, J. A.; Tse, J. S.; Dahn, J. R.; Lee, F.; Calvert, L. D. *Mol. Cryst. Liq. Cryst.* **1986**, *141*, 141−149.
(30) Roberts, R. B.; Andrikdis, C.; Tainsh, R. J.; White, G. K. *Proceedings of ICEC-10*, Helsinki, 1984.
(31) Röttger, K.; Endriss, A.; Ihringer, J.; Doyle, S.; Kuhs, W. F. *Acta Crystallogr.* **1994**, *B50*, 644−648.
(32) Büeler, B.; Enge, A.; Fukuda, K. Exact volume computation for polytopes: A practical study. In *Polytopes—Combinatorics and Computation*; Kalai, G., Ziegler, G. M., Eds.; DMV Seminars Vol. 29; Birkhäuser Verlag: Basel, Switzerland, 2000.
(33) Gutt, C.; Asmussen, B.; Press, W.; Johnson, M. R.; Handa, Y. P.; Tse, J. S. *J. Chem. Phys.* **2000**, *113* (11), 4713−4721.
(34) Jones, W.; March, N. H. Perfect Lattices in Equilibrium. *Theoretical Solid State Physics*; New York: Wiley 1973; Vol. I, pp 286−293.
(35) Udachin, C. K. A.; Ratliffe, C. I.; Ripmeester, J. A. *J. Phys. Chem. B* **2001**, *105*, 4200−4204.
(36) Tse, J. S.; McKinnon, W. R.; Marchi, M. *J. Phys. Chem.* **1987**, *91*, 4188−4193.
(37) Tanaka, H.; Tamai, Y.; Koga, K. *J. Phys. Chem. B* **1997**, *101*, 6560−6565.